Cell Cycle Blockade and Differentiation of Ovarian Cancer Cells by the Histone Deacetylase Inhibitor Trichostatin A Are Associated with Changes in p21, Rb, and Id Proteins[1]

Kevin A. Strait,[2] Bashar Dabbas, Elizabeth H. Hammond, C. Terry Warnick, Sarah J. Ilstrup, and Clyde D. Ford

Departments of Medicine [K. A. S., C. D. F.] and Pathology [B. D., E. H. H., C. T. W., S. J. I.], Cancer Research Laboratory, LDS Hospital, Salt Lake City, Utah 84143

Abstract

Inhibitors of histone deacetylase activity are emerging as a potentially important new class of anticancer agents. In the current studies, exposing A2780 ovarian cancer cells to the histone deacetylase inhibitor trichostatin A (TSA) produced a marked change in cellular morphology, proliferation, and differentiation. Within 24 h of TSA treatment, there was a morphological transformation of the cells, with increased cytoplasm, a more epithelial-like columnar appearance, and the emergence of distinct cellular boundaries. Commensurate with the morphological transformation, TSA also inhibited cell proliferation; cells treated with TSA for 72 h increased to 110% of the initial cell numbers *versus* control cell numbers of 622%, with a corresponding reduction in mitotic activity and a flow cytometry S-phase fraction of 3.9% in TSA-treated cells *versus* 28.8% for control. TSA also induced epithelial-like differentiation with increased cytokeratin expression from 2% of controls to 22–25% of TSA-treated cells and the reappearance of intercellular plasma membrane junctions and primitive microvilli. Immunocytochemical analyses indicate the molecular mechanism underlying the actions of TSA on A2780 cell cycle progression and differentiation involves reexpression of the CDK inhibitor p21. Elevated levels of p21, in TSA-treated cells, were associated with a reduction in the phosphorylation of the cell cycle regulator retinoblastoma protein (Rb). TSA also caused a decrease in the helix-loop-helix inhibitor of differentiation/DNA binding protein Id1, with no change in Id2 levels. In conclusion, the observed TSA-induced changes in p21, Rb, and Id1 are consistent with cell cycle senescence and differentiation of A2780 ovarian cancer cells.

Introduction

Ovarian cancer is the leading cause of gynecological cancer deaths in the United States (American Cancer Society). The vast majority of these cancers (85%) arise from specialized epithelial cells that cover the surface of the ovary (1). Over the past several years, a number of important oncogenes and oncosuppressor genes have been identified whose activities are linked to tumorigenesis. Many of these genes are aberrantly expressed or silenced in cancer cells due to widespread epigenetic modifications of the tumor cell genome (2). Because complex cellular processes involving the cell cycle, differentiation, and apoptosis often have overlapping pathways, identifying individual control genes or gene products for targeted therapies is difficult.

The recent identification of gene-regulatory chemotherapeutic agents that can reverse the epigenetic modifications present in the tumor cell genome is an area of intensive investigation (3). One mechanism through which the activity of multiple genes can be affected is modification of the structure of the DNA chromatin complex. In particular, post-translational modifications of the core histone proteins that comprise the nucleosomal complex are known to dramatically influence the transcription of genes in response to cellular signals (4). Recent interest has focused on the acetylation of the histone proteins, which neutralizes their net positive charge, leading to a loosening of the histone-DNA nucleosomal structure (5) and increased transcriptional activity (4).

The net acetylation state of histones is the function of diametrically opposed histone acetyltransferase and HDAC[3] enzyme families. Histone acetyltransferases have been identified as transcriptional coactivators in a number of species (6, 7). Conversely, HDACs have been shown to interact with several known transcriptional repressors, including Sin3, SMRT, and NCoR, where they function as corepressors (8). Changes in histone acetylation via recruitment of HDAC enzymes appear to be targeted to specific genes because microarray analysis of mRNA expression profiles indicate that HDAC inhibitors affect a small percentage (1–2%) of the total genes expressed (9).

The association of HDAC activity with known cellular oncogenes has led to speculation that histone deacetylation is a potential mechanism to account for the uncontrolled cell proliferation associated with cancers. Support for this hypothesis was provided in studies of acute promyelocytic

Received 6/12/02; revised 8/22/02; accepted 9/13/02.
[1] Supported by grants from Feature Films for Families Cancer Research Fund (CEO, Forrest S. Baker III) and The Deseret Foundation.
[2] To whom requests for reprints should be addressed, at Cancer Research Laboratory, Department of Medicine, LDS Hospital, 325 8th Avenue, Salt Lake City, UT 84143. Phone: (801) 408-1558; Fax: (801) 408-5822, E-mail: ldkstrai@ihc.com.

[3] The abbreviations used are: HDAC, histone deacetylase; EM, electron microscopy; TSA, trichostatin A; RA, retinoic acid; CDK, cyclin-dependent kinase; HLH, helix-loop-helix.

leukemia cells, where a fusion protein of PML and a RA receptor repressed gene transcription by recruiting HDAC enzymes (10). PML-RA receptor fusion protein recruitment of HDAC produced sustained cell proliferation that was resistant to the differentiation actions of RA (10). Pretreating these cells with HDAC inhibitors relieved the transcriptional blockade and allowed them to undergo normal differentiation (11).

Given the close association between HDAC activity and repression of transcription in tumors, inhibitors of HDAC are emerging as a potentially important new class of anticancer agents. TSA is a potent specific inhibitor of HDAC activity through a mechanism that involves Zn+ ion chelation (12). In the past several years, studies have shown that TSA induces growth arrest, differentiation, and/or apoptosis in a number of cancers, including breast (13), colon (14), lung (15), and leukemic cells (16).

How TSA's inhibition of HDAC activity leads to cell cycle arrest and differentiation is an area of intense investigation. Several reports indicate that HDAC inhibitors block cell cycle progression by reexpressing inhibitors of the CDKs, such as p21 (17). p21 inhibition of CDK activity blocks cell cycle progression by inducing hypophosphorylation of the CDK substrate retinoblastoma protein (Rb; Ref. 18). Hypophosphorylation of Rb blocks cell cycle progression by binding and sequestering cell cycle control factors, including the transcription factor E2F (19).

Another group of proteins associated with the morphogenesis of several cell types, including epithelial cells, are the inhibitors of differentiation/DNA binding proteins (Id proteins; Ref. 20). The Id proteins belong to the basic HLH family of transcription factors, characterized by their ability to form dimmers through interaction of their basic HLH regions and bind response element sequences via a DNA-binding domain (21). The Id proteins (Id1–4) are structurally and biologically distinct from the other HLH proteins in that they lack a DNA-binding domain (22). As such, they function as negative regulators of the other HLH proteins through the formation of heterodimers that are unable to bind DNA, and they play an essential role in embryogenesis by stimulating cell proliferation and inhibiting premature differentiation (21). Given their effects on proliferation and differentiation, recent studies have focused attention on their potential role in cancer, where an association between the loss of appropriate regulation of Id expression and tumorigenesis has emerged (23).

In the present studies, we examined the effects of TSA on the morphology, proliferation, and differentiation of A2780 ovarian cancer cells. Our data indicate that TSA caused a significant alteration in cellular morphology, the result of inhibition of cell cycle progression and stimulation of epithelial-like differentiation. Immunocytochemical analyses indicated that the morphological, proliferative, and differentiation effects of TSA occur commensurate with changes in p21, Rb, and Id, consistent with an important role for these proteins in the observed cell cycle inhibition and epithelial-like differentiation.

Materials and Methods

Cell Culture and Reagents. The human ovarian cancer cell line A2780 was obtained from the European Collection of Cell Cultures (Salisbury, United Kingdom). A2780 cells were cultured in RPMI 1640 supplemented with 10% fetal bovine serum. Cultures were grown at 37°C in a humid 95% air:5% CO_2 chamber and periodically tested to ensure they remained free of *Mycoplasma* infection during the course of the experiments. TSA was obtained from Sigma (St. Louis, MO).

TSA Treatment. Twenty-four h before TSA addition, A2780 cells were subcultured onto either fresh 100-mm tissue culture plates or Lab-Tek chamber slides. The following day, the media were replaced with fresh media containing 100 ng/ml TSA, and the cells were allowed to incubate overnight. The following day, the TSA was removed by replacing the media, and the cells were again returned to the incubator for an additional 24–48 h. At various times during the experimental period (as noted), cells were removed from the plates or fixed to the Lab-Tek slides and examined for TSA-induced changes.

Preparation of Paraffin Blocks from Cultured Cells. Cultured A2780 cells were fixed and embedded in paraffin blocks as described previously (24). Briefly, cultures were trypsinized and removed from the culture dishes upon dilution with 2 volumes of media +10% FBS, centrifuged at 150 $\times$ *g* for 5 min, washed once in culture medium to remove the excess trypsin, and recentrifuged. The final pellet was resuspended in 0.25 ml of medium, and 0.5 ml of human plasma was added, followed by a similar volume of thromboplastin, as described previously (25). The mixture was agitated for 2 min until coagulation occurred, followed by addition of 10% buffered formalin for 2 min. The clotted sample of cells was removed, placed in a VIP Tissue Processor (SAKURA), and allowed to process overnight. The following day, the processed sample was embedded in a paraffin block, and 4-μm sections were cut and mounted on slides.

H&E Staining. Cells grown on microscope slides (Lab-Tek) were washed twice with PBS, fixed with 4% paraformaldehyde (5 min, room temperature), dehydrated through a series of ethanol washes, and stained with H&E (26).

Immunohistochemistry. Paraffin-embedded fixed cells were immunostained for Ki67, CAM 5.2, or AE1/AE3. Immunostaining of p53, p21, p27, Rb, and Id proteins was performed on cells grown on Lab-Tek chamber slides and fixed in 100% methanol for 10 min. Both paraffin-embedded and methanol-fixed cells were stained using an immunoperoxidase procedure, as described previously (27) with 3,3′-diaminobenzidine as the substrate. Staining was performed on a DakoAutoStainer (DAKO). Briefly, mouse monoclonal antibodies against human Ki67 (DAKO; 1:10 dilution); CAM 5.2 (Becton Dickinson; prediluted); AE1/AE3 (DAKO; prediluted); p53 (DAKO; 1:200); $p21^{WAF1/Cip1}$ (DAKO; 1:50); $p27^{Kip1}$, Rb, and Phos-Rb (ser 795; Cell Signaling Technology; 1:100 dilution); and Id1 and Id2 (Santa Cruz Biotechnology; 1:200 dilution) were used as the primary antibody. The secondary antibody was a biotinylated goat antimouse antibody (DAKO; prediluted). Antibody binding was detected using horseradish peroxidase (LSAB2 System; DAKO). The following control tissues were stained simultaneously to act as positive controls for the antisera: Ki67 (tonsil); AE1/AE3 (squamous cell carcinoma of skin); p21 (colon); p27 (tonsil);

and p53 (p53 positive tumor). For the Rb and Id antisera, control A2780 cells were included on each slide to act as positive controls. The samples were counterstained with hematoxylin (DAKO), dehydrated, and mounted. The percentage of positively stained cells was determined from five separate areas of the slide using an automated cell imaging system (Chromavision). The automated cell imaging system combines automated microscopy to record and assemble hundreds of individual captured fields with computerized image analysis to simultaneously determine both staining intensity and percentage of stained cells for control and TSA-treated cells on the same slide.

Flow Cytometry. The percentage of cells in G_1, S, and G_2-M phase of the cell cycle was determined by a modified Vindelov propidium iodide DNA staining procedure (28). Briefly, cells were isolated from the culture dishes with trypsin, washed once in fresh media, and resuspended at a concentration of 1×10^6 cells/ml. The cell suspension (200 μl) was then incubated with 500 μl of a propidium iodide solution [0.006 g of PI, 70 units of RNase, 0.058 g of NaCl, 0.121 g of Trisma base, and 0.1 ml of NP40; volume to 100 ml (pH 8.0)] overnight at 4°C. The following day, the stained cell nuclei were run on a Coulter Epix XL flow cytometer. The ungated histogram was evaluated using the Phoenix flow DNA modeling system to determine the percentage of cells in G_1, S, and G_2-M phase.

EM. Cells were fixed and sectioned for EM as described previously (29). Briefly, cultured cells were rinsed twice in 5 ml of PBS and then gently scraped from the cultures plates in 1 ml of PBS using a Teflon cell scraper. The cells were spun at 1000 rpm (5 min) to form a cell pellet in the bottom of a 15-ml conical tube. The supernatant was removed and carefully replaced with 1 ml of 4% glutaraldehyde so as not to disrupt the pellet and allowed to fix for 1.5 h. The fixed cell pellet was then washed twice in PBS for 30 min, followed by the addition of 2 ml of 2% Osmium and an additional 30-min incubation. The pellet was again rinsed twice (10 min) in normal saline, dehydrated stepwise with acetone (30%, 70%, 95%, and 100%; 5 min each), and embedded in an epoxy resin (Embed) at room temperature in a 1:1 dilution of acetone:Embed for 15 min. The excess solution was removed, and the pellet was embedded in a Beem capsule and allowed to polymerize overnight at 85°C. The polymerized cell pellets were subsequently sectioned on an Ultratome (LKB), affixed to 200 mesh copper grids, stained with uranyl acetate and lead citrate, and examined on the JEM1010 JEOL electron microscope.

Results

Previous studies using inhibitors of HDAC in other cancers indicate that these compounds reduce cell proliferation and induce differentiation or apoptosis. Therefore, we initially examined whether addition of the HDAC inhibitor TSA to A2780 cultures produced any effect on cellular morphology. Fig. 1 is a photomicrograph composite of A2780 cells incubated in the presence (100 ng/ml, 24 h) or absence (control) of TSA. Control A2780 cells (Fig. 1, *left panels*) appear as undifferentiated small round clumps of cells with indistinct cell borders. Examining these same cells on successive days

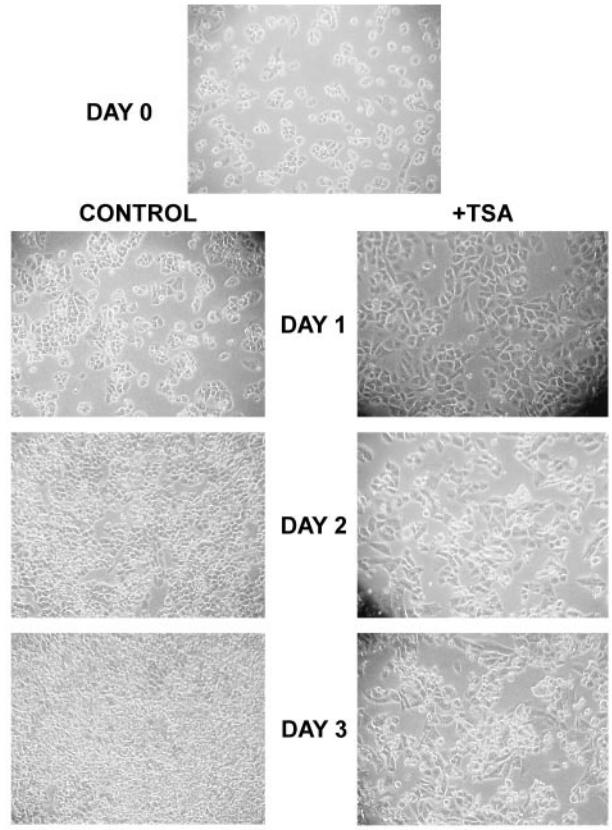

Fig. 1. Phase-contrast photomicrograph of A2780 cells ± TSA. A2780 cells were grown in culture dishes in the absence (control) or presence of TSA (100 ng/ml; 24 h) and then followed for 3 days. Photomicrographs were taken of cells growing in the culture dishes using an inverted phase-contrast microscope. Day 0 cells are before TSA treatment. Days 1–3 cells: *left panels,* control; *right panels,* +TSA. The photomicrographs presented are representative of three independent experiments with similar results (original magnification, ×100).

indicated that they remained undifferentiated and were rapidly dividing, reaching confluence by the third day.

Photomicrographs in the *right panels* of Fig. 1 (+*TSA*) show the same A2780 cells treated with TSA (100 ng/ml, 24 h). As is apparent from the figure, within 24 h, TSA had a dramatic effect on the morphology of the cells. The original small round clumps of cells (day 0) spread out in monolayer on the surface of the plate. There was an increase in the amount of cytoplasm, with the appearance of numerous cytoplasmic projections and well-defined cellular borders. Examining the cells 24–48 h after removal of TSA (days 2 and 3) showed a persistent effect of TSA on morphology.

H&E staining (Fig. 2) of the cells confirmed the morphological changes observed using phase-contrast microscopy. Cells were stained on day 0 and on day 2, after ±TSA treatment. Control A2780 cells appear as small, round, undifferentiated cells that grow in clusters, with round to slightly oval nuclei and very little cytoplasm. A majority of the TSA-transformed cells had a significant increase in cytoplasmic content, resulting in a stellate-like appearance, often with multiple cytoplasmic projections radiating out from the cell body and well-defined nuclei with prominent nucleoli. TSA-

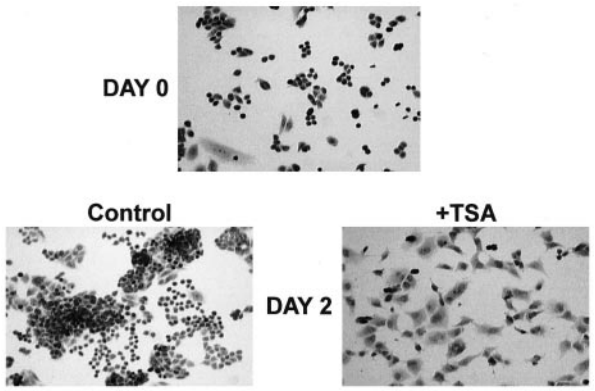

Fig. 2. H&E staining of A2780 cells ± TSA. A2780 cells were grown on Lab-Tek chamber slides in the absence (control) or presence of TSA (100 ng/ml; 24 h). Slides were fixed on day 0 and on day 2 and stained as described in "Materials and Methods." Photomicrographs were taken to record changes in morphology over the 2-day experimental period. Day 0 cells are before TSA treatment. Days 2 cells: *left panel,* control; *right panel,* +TSA. The photomicrographs presented are representative of two independent experiments with similar results (original magnification, ×200).

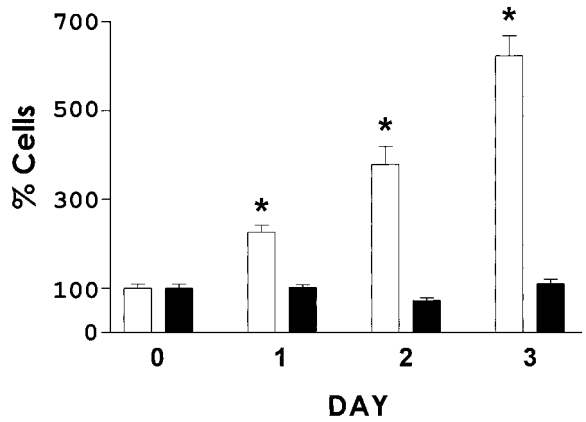

Fig. 3. TSA inhibition of *in vitro* A2780 cell growth. A2780 cells were grown in culture dishes in the absence (control; □) or presence of TSA (■; 100 ng/ml, 24 h) and followed for 1–3 days. Cells were counted at the indicated times using a hemocytometer and trypan blue exclusion. Cell counts are the average from three separate plates after trypsin-mediated detachment from the culture dishes. Day 0 cells were before TSA addition. Data are presented as the mean ± SD of triplicate values from a typical experiment. Statistical significance ($P < 0.05$) was determined by ANOVA. ∗ indicates a significant difference in the number of cells as compared with day 0.

treated cultures also had a significantly reduced cell density as compared with control cultures.

To test whether the reduced cell density after TSA treatment is the result of changes in proliferation or apoptosis, we determined both the cell numbers and viability of our TSA-treated cultures (Fig. 3). As indicated in the figure, TSA addition to the media affects the proliferation of the A2780 cells, producing a significant ($P < 0.05$) reduction in cell numbers within the first 24 h [+TSA; 105 ± 13% of the starting cell numbers as compared with control cells (226 ± 23%)] that persisted for at least another 48 h after TSA was removed from the culture medium [day 3: 110 ± 12% (TSA) and 622 ± 37% (control; $P < 0.01$)]. The difference in cell numbers in control *versus* TSA-treated cultures is directly attributable to a complete cessation of cell proliferation in the TSA-treated cultures over the entire 3-day experimental period (initial cell numbers = 100; +TSA: day 1, 105%; day 2, 84%; and day 3, 110%).

To determine whether the reduction in the number of cells in the TSA-treated cultures was the result of an increase in apoptotic cell death, we examined both the cell culture medium and the trypsinized cells for viability using trypan blue exclusion. At no time in the 3-day experimental period did we observe a loss of cells in the TSA-treated cultures, due either to dissociation from the culture dish or decreased cell viability, in excess of that observed in the A2780 control plates (<1% of cells; data not shown). In addition, we also stained control and TSA-treated cells with annexin V to identify phosphatidylserine translocation to the external plasma membrane, an early event in apoptosis. In two separate experiments, annexin V bound to <1% of the cells in both the control and TSA-treated cultures (data not shown).

Evidence to support a TSA-mediated arrest in A2780 cell proliferation was obtained by immunohistochemical analysis, using an antibody (Ki67) that only stains mitotically active cells (Fig. 4). In control cultures, Ki67 stained nearly all of the cells (89.7 ± 2.1%). By contrast, the presence of TSA in the media resulted in a significant ($P < 0.01$) reduction in the levels of Ki67 staining to 54 ± 7.5% of the cells.

Flow cytometry analysis of propidium iodide-stained cells indicated that TSA's inhibition of A2780 proliferation is the result of cell cycle blockade (Fig. 5). The histogram of DNA content in the control cultures (Fig. 5*A*) showed a majority of cells in G_1 (55.0%), with a significant S-phase fraction of 28.8%. The remaining control cells (16.2%) were found to be in G_2-M phase. TSA treatment produced a shift in the DNA content histogram (Fig. 5*B*). Whereas the G_1-phase fraction remained essentially unchanged after TSA treatment (59.2%), the S-phase fraction decreased significantly ($P < 0.01$) to 3.9%. The decrease in the S-phase fraction was offset by a rise in the G_2-M-phase fraction (36.9%), the result of an arrest in the cell cycle at the G_2-M checkpoint.

To examine whether the changes in morphology and proliferation documented above are a reflection of cell differentiation, we examined our A2780 cultures for expression of genes associated with an epithelial phenotype. Control and TSA-treated cells were immunostained with antibodies (AE1/AE3 and CAM 5.2) directed against several cytokeratin proteins (Fig. 6). As anticipated, control A2780 cells were virtually devoid of cytokeratin staining (2% of cells showed weak immunoreactivity against either antisera). TSA treatment triggered reexpression of the cytokeratins, with immunostaining increasing significantly ($P < 0.01$) to 22% (AE1/AE3) and 25% (CAM 5.2) of cells.

Control and TSA-treated cells were further examined ultrastructurally to look for subcellular changes commensurate with epithelial-like differentiation (Fig. 7). Photomicrographs of control A2780 cells (Fig. 7*A*) show that the plasma membranes of adjacent cells abut without forming intercellular junctions (Fig. 7*A*, *open arrow*). Occasional intercellular luminal spaces were present (labeled *L*), which contained rare,

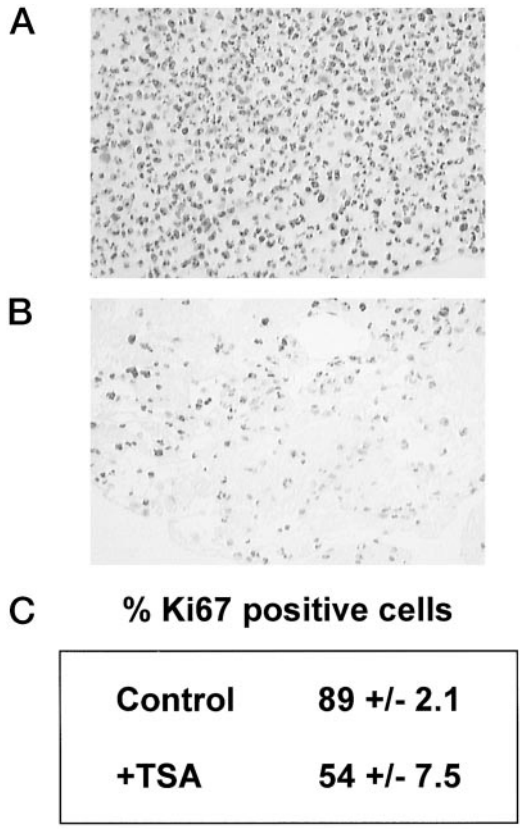

Fig. 4. TSA decreases Ki67 staining in A2780 cells. *In vitro* cultures of A2780 cells were treated with the absence (control) or presence of TSA (100 ng/ml, 24 h). On day 2, the cells were removed from the culture dishes with trypsin, pelleted, formalin fixed, paraffin embedded, and stained for the presence of the Ki67 antigen (see "Materials and Methods"). The photomicrographs are representative of two independent experiments and show the presence of Ki67 staining as *punctate brown dots* located within the nuclei of A2780 cells from control (*A*) and TSA-treated (*B*) cultures. The percentage of cells staining for Ki67 was determined by counting five separate areas of each slide using a Chromavision automated cell imaging system. Data are presented as means ± SD. Significance ($P < 0.05$) was determined by unpaired Student's test (original magnification, ×200).

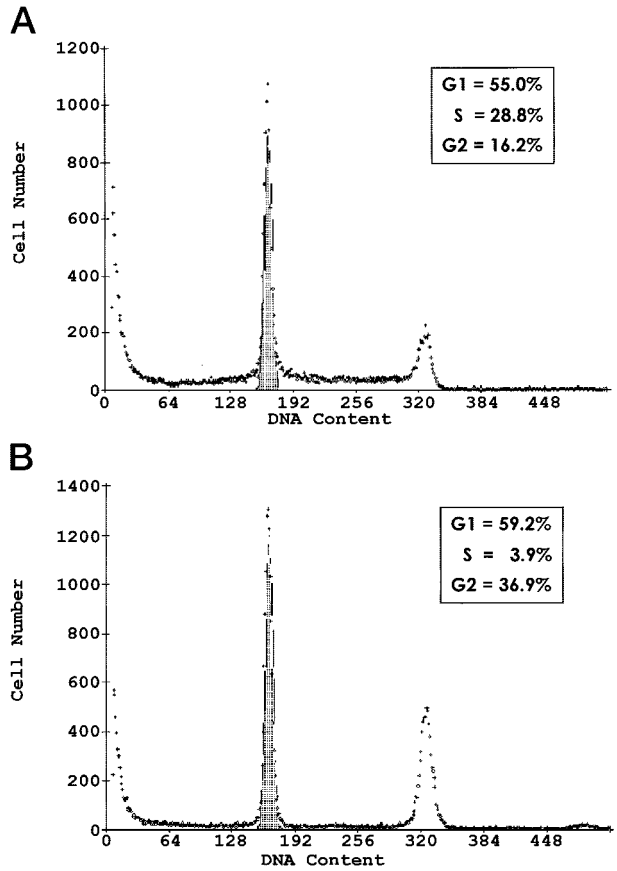

Fig. 5. Induction of A2780 cell cycle arrest by TSA. *In vitro* cultures of A2780 cells were treated with the absence (*A*) or presence (*B*) of TSA (100 ng/ml, 24 h). On day 2, the cells were removed from the culture and analyzed by fluorescence-activated cell sorting for cell cycle distribution. A representative histogram from three independent experiments is shown. *Insets* show the percentage of cells in each phase of the cell cycle (G_1, S, and G_2-M). The coefficient of variance for G_1, S, and G_2-M ranged from 1.8 to 2.2.

abortive microvilli. After treatment with TSA (Fig. 7*B*), intercellular junctional fusions were clearly present between adjacent cells (*filled arrows*), resembling zona occludens. In addition, the intercellular luminal spaces (labeled *L*) were more frequent and contained primitive, epithelial-like surface microvilli.

Having established that TSA induced cell cycle arrest and differentiation, we refocused our studies to investigate potential mechanisms underlying the actions of TSA. Control and TSA-treated cells were examined for the presence of selective inhibitors of cell cycle progression (Fig. 8). TSA treatment caused a marked fall in p53 expression within 24 h, from 52% of control cells to 8% of TSA-treated cells ($P < 0.05$). p21 (Waf1/Cip1) expression in similarly treated cells increased significantly ($P < 0.01$) from the weak signal present in only 11% of control cells to intense immunostaining in 84% of TSA-treated cells. Immunostaining for another inhibitor of CDK activity, p27/Kip 1, showed no significant difference in control (76%) and TSA-treated (69%) cells, an indication that the effects of TSA on p21 expression were not due to a generalized increase in all CDK inhibitors.

Because p21 is an inhibitor of CDK-mediated phosphorylation, we examined the effects of TSA on the phosphorylation status of a CDK substrate involved in cell cycle regulation, the Rb protein (Fig. 9). Immunostaining of A2780 cells with an antibody that recognizes the Rb protein only when phosphorylated at serine 795 [Fig. 9, *Rb(795)*] was significantly diminished in TSA-treated cells (28%) compared with controls (77%; $P < 0.05$), with a concomitant 60% reduction in the intensity of staining. To ensure that the loss of immunostaining was the result of a reduction in Rb phosphorylation, we stained similarly treated cells with an antibody capable of detecting total Rb protein regardless of phosphorylation status (Fig. 9, *Rb*). These experiments confirmed that total Rb protein was unaffected by TSA treatment as determined by similar immunoreactivity in 82% of control cells and 81% of TSA-treated cells.

We also examined TSA-treated cells for expression of the Id proteins (Fig. 9), which have previously been shown to play

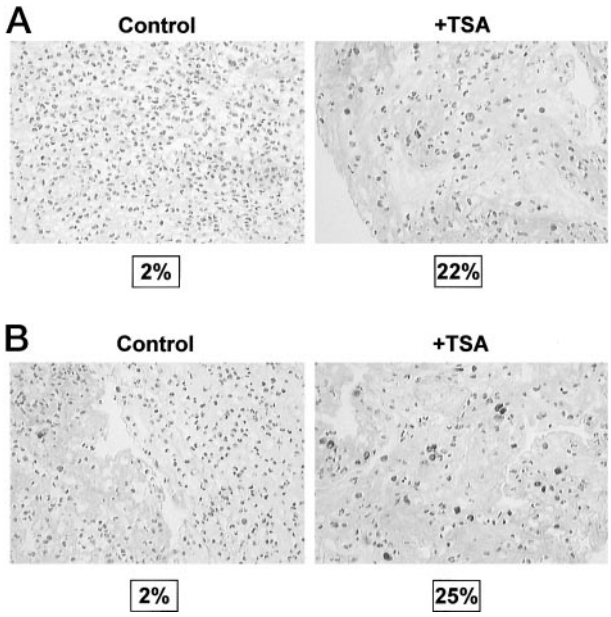

Fig. 6. TSA induces reexpression of cytokeratin proteins in A2780 cells. A2780 cells treated ± TSA (48 h) were removed from the culture dishes with trypsin, pelleted, formalin fixed, paraffin embedded, sectioned, and stained (see "Materials and Methods"). Control (*left panels*) or TSA-treated (*right panels*) cells were stained for cytokeratin proteins using antibodies AE1/AE3 (*A*) and CAM 5.2 (*B*). The percentage of cells staining for AE1/AE3 and Cam 5.2 are shown in *boxes* below the photomicrographs. The percentage of positively stained cells was determined by counting five separate areas of each slide using a Chromavision automated cell imaging system. [AE1/AE3 staining: control, 2 ± 1.8%; +TSA, 22 ± 6.9%; CAM 5.2 staining: control, 2 ± 0.9%; +TSA, 25 ± 4.5%]. Data are presented as means ± SD. Significance ($P < 0.05$) was determined by unpaired Student's *t* test. The figure is representative of three independent experiments with similar results (original magnification, ×200).

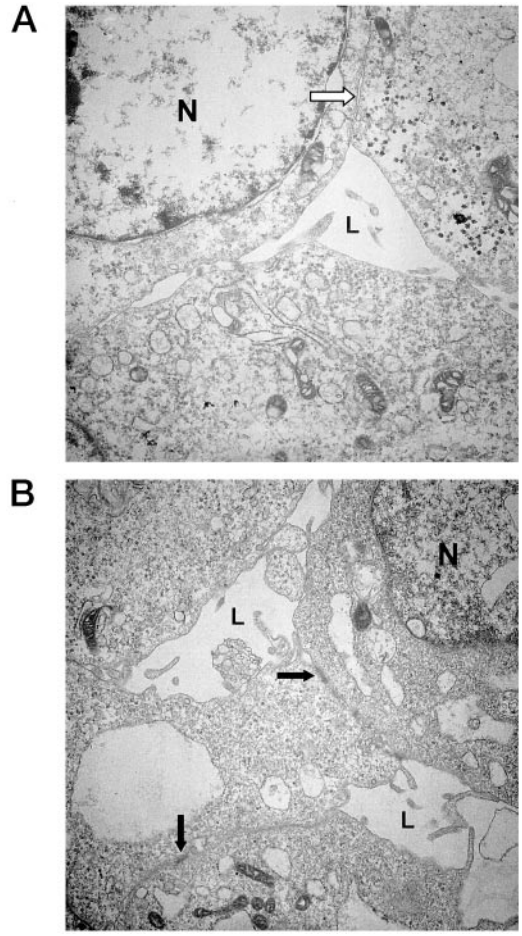

Fig. 7. Ultrastructural analysis of intercellular junctions. A2780 control (*A*) or TSA-treated (*B*) cells were fixed and examined for intercellular junctions using EM. Cells were treated ± TSA for 24 h, the media were changed to remove residual TSA, and then cells were incubated for an additional 24-h period (day 2) before EM. *Arrows* indicate junctions between the plasma membranes of adjacent cells (*open arrow,* control cells; *filled arrow,* TSA-treated cells). The luminal spaces formed between cells are denoted in the photomicrograph (*L*). As a point of reference, nuclei are also labeled *N*. Original sample magnification was ×4000. The photomicrographs are representative of two independent experiments with similar results.

a critical role in cell cycle regulation and the normal cellular differentiation of a number of cell types, including epithelial cells (30). In control A2780 cells, Id1 protein was abundantly expressed with intense nuclear staining in >82% of the cells. TSA significantly reduced Id1 expression to 28% of the cells ($P < 0.05$), with a 70% reduction in the intensity of staining. Similar staining with an Id2-specific antibody also showed high levels of expression in the control cells (92%); however, there was no effect of TSA on Id2 expression (85%, TSA-treated cells).

Discussion

The present studies provide evidence that alterations in histone acetylation have a dramatic effect on the proliferation and differentiation of ovarian cancer cells. In the current studies, within 24 h of TSA exposure, A2780 cells demonstrated measurable changes in both cellular morphology and proliferation (Figs. 2 and 3). Diminished proliferation of ovarian cancer cell lines has previously been reported using aromatic fatty acid analogues as inhibitors of HDAC activity (31). In the present studies, we have extended this observation to show that diminished proliferation is the result of a reduction in the S-phase fraction [28.8% (control) *versus* 3.9% (TSA-treated cells); Fig. 5] due to cell cycle blocks at the G_1 and G_2-M checkpoints, consistent with an association between HDAC activity and cell cycle control genes (32).

Our studies also provide evidence that TSA may produce cell cycle blockade through a mechanism that involves the p21 Rb/E2F cell cycle-regulatory system. Treating A2780 cells with TSA causes an increase in the CDK inhibitor p21, by a p53-independent mechanism (Fig. 8). Commensurate with p21 inhibition of CDK activity, we observed a measurable reduction in phosphorylated Rb protein (serine 795) in TSA-treated cells, with no change in total Rb protein (Fig. 9). The significance of a change in the phosphorylation state of Rb relates to its ability to bind the cell cycle control factor E2F. CDK phosphorylation of Rb, at any of several sites within the large A/B pocket region (including serine 795), prevents Rb binding to E2F (33), allowing E2F to stimulate cell cycle progression. By analogy, in TSA-treated A2780

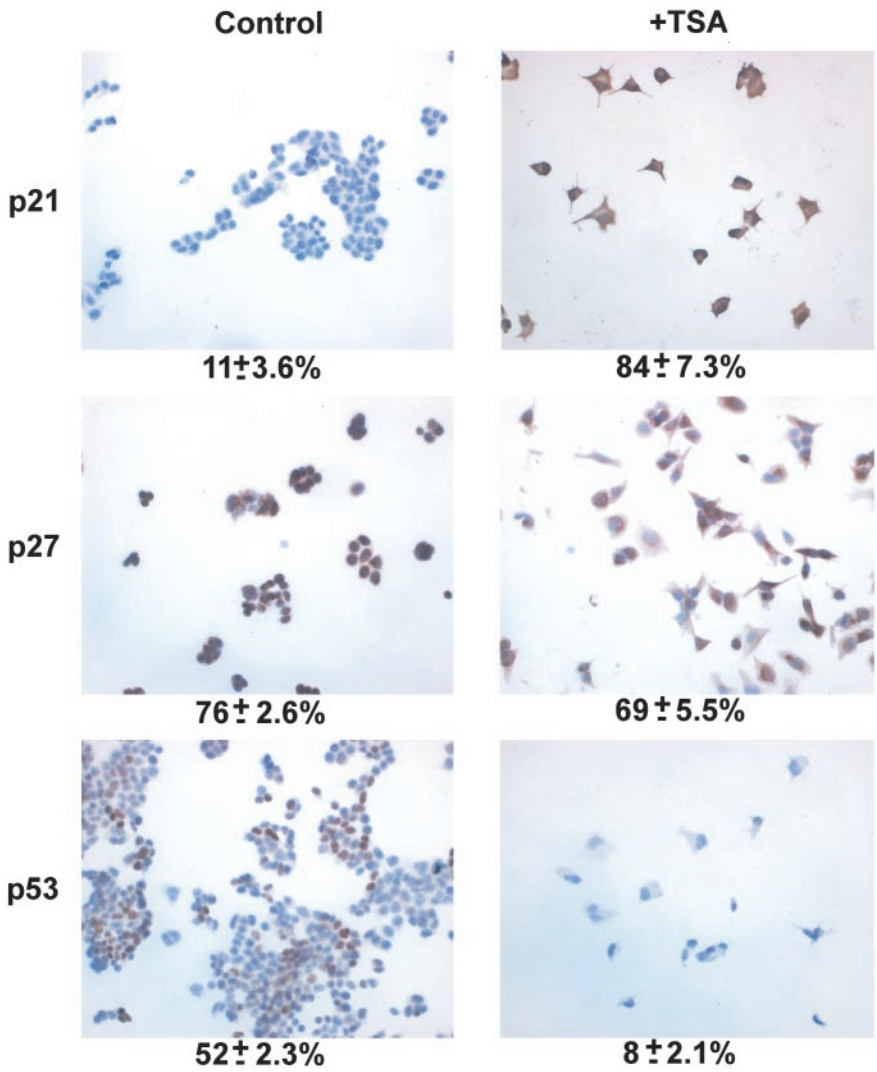

Fig. 8. TSA-mediated changes in cell cycle inhibitor proteins. A2780 control (*left panels*) and TSA-treated (*right panels*) cells were stained for the cell cycle-regulatory proteins p53, p21, and p27 as described in "Materials and Methods." A representative photomicrograph of each antisera's staining is presented, with the percentage of positively stained cells shown *below* each photomicrograph. The percentage of positively stained cells was determined by counting five separate areas of each slide using a Chromavision automated cell imaging system. Data are presented as means ± SD. Significance ($P < 0.05$) was determined by unpaired Student's *t* test. The figure is representative of three independent experiments with similar results (original magnification, ×200).

cells, diminished phosphorylation of Rb would increase Rb-E2F binding, resulting in the observed cell cycle arrest (Fig. 5).

The current studies also provide the first demonstration that TSA down-regulates the expression of Id1, one of the inhibitors of differentiation/DNA binding proteins, with no change in Id2 levels (Fig. 9). A number of tumors exhibit aberrant expression of the Id genes (23). Evidence indicates that reducing Id1 protein expression results in suppression of cell proliferation (34), whereas overexpression of Id1 prevents cell cycle arrest and differentiation (35). These observations are in accord with our present findings that Id1 expression falls in A2780 cells after TSA exposure, commensurate with cell cycle blockade and differentiation (Fig. 9).

The role the various Id proteins play in regulating the activity of HLH proteins during normal cell cycle progression and differentiation is presently unknown. However, among the Id proteins, Id1 is unique in that it alone can bind to mouse Id-associated protein 1 (36). Id1 binding facilitates the interaction of mouse Id-associated protein 1 with DNA elements within the promoter region of several known growth factor/cytokine genes, inducing their expression to stimulate cell proliferation (36). Other data indicate that Id1 may also directly stimulate cell proliferation by binding the HLH transcription factor E2A, rendering E2A incapable of inducing the expression of the cell cycle inhibitor p21 (37). Thus, in the present studies, the fall in Id1 expression in TSA-treated A2780 cells is consistent with the observed increase in p21 expression (Fig. 8) and the reduction in cell proliferation (Fig. 5). Finally, the fall in Id1 expression occurs commensurate with epithelial-like differentiation (Figs. 6 and 7) and might indicate that Id1 functions as an inhibitor of ovarian epithelial cell differentiation, similar to reports in other cell lines (21), by sequestering HLH-containing transcription factors necessary for the expression of genes associated with a terminally differentiated phenotype.

In A2780 cells, Id2 proteins were unaffected by TSA (Fig. 9). The disparity in Id1 *versus* Id2 protein responses to TSA may relate to recent data that indicate these proteins appear to be functionally distinct (38). Id2 proteins, but not Id1, are

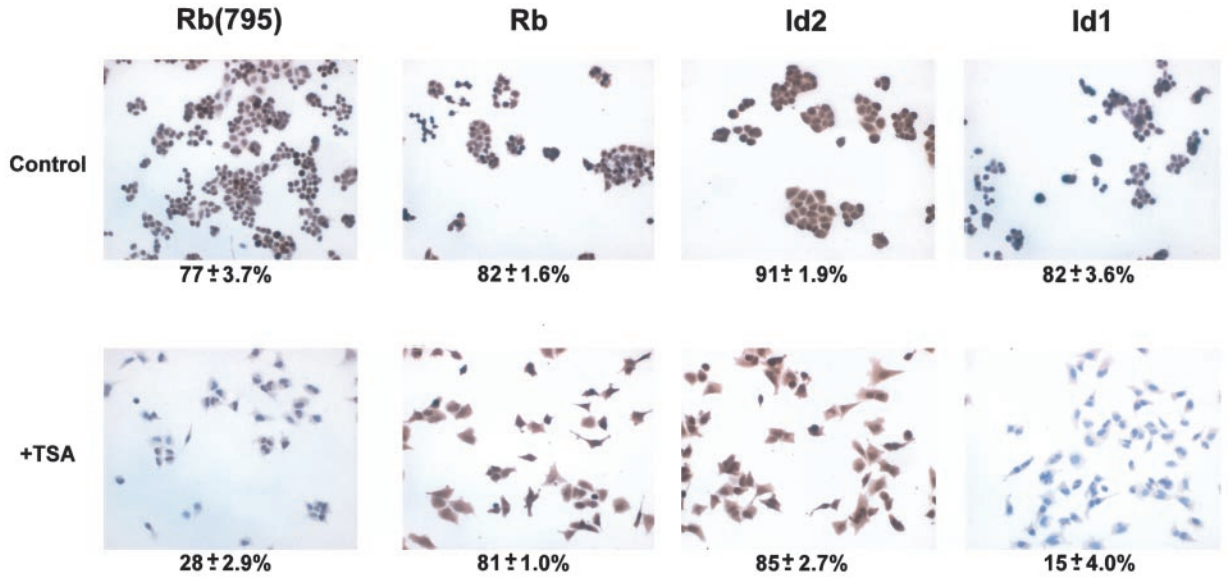

Fig. 9. TSA affects Rb phosphorylation and expression of the inhibitors of differentiation and DNA binding proteins (Id proteins). A2780 control and TSA-treated cells were stained using antibodies directed against Rb, Id1, and Id2 proteins. Rb antiserum recognizes the Rb protein regardless of phosphorylation state; Rb(795) antiserum only binds to Rb proteins containing a phosphorylated serine residue at amino acid 795. The percentage of cells staining for the Rb, Rb(795), Id1, and Id2 are shown immediately *below* the photomicrographs. The percentage of positively stained cells was determined by counting five separate areas of each slide using a Chromavision automated cell imaging system. Data are presented as means ± SD. Significance ($P < 0.05$) was determined by unpaired Student's *t* test. The figure is representative of three independent experiments with similar results (original magnification, ×200).

able to disrupt HLH-containing proteins from binding to the E-box sequences of promoters from genes involved in the G_1 to S-phase transition (39). In this same series of experiments, the Id2 protein was also shown to be a substrate for phosphorylation by the G_1-specific CDK2 enzyme, which was not able to phosphorylate Id1 (39). The use of mutant Id2 isoforms, which are incapable of being phosphorylated by CDK2, indicates that phosphorylation blocks Id2 binding to proteins involved in cell cycle regulation, analogous to phosphorylation of Rb by CDKs, and is required for cell cycle progression through the G_1-S checkpoint (39). Therefore, in TSA-treated A2780 cells, it appears plausible that p21 inhibition of CDK activity also produces hypophosphorylated Id2 proteins, which facilitate cell cycle blockade by Rb by sequestering additional cell cycle control factors.

Id2 proteins may also play a role in A2780 cell differentiation; however, unlike the Id1 proteins that block differentiation, the available data indicate that Id2 proteins facilitate terminal differentiation (21). For example, in myeloid cells, the presence of Id2 protein was shown to be an absolute requirement for differentiation (40, 41). Particularly relevant to the present studies, in which Id2 proteins remain elevated during TSA-mediated cell cycle inhibition/differentiation, studies using antisense transcripts have shown that Id2 expression was essential for normal mammary epithelial cell differentiation (42). In these same cells, differentiation was accompanied by a fall in Id1 (42) that overexpression studies indicated was required for the cessation of cell proliferation and induction of differentiated phenotypic gene expression (42). Thus, the presence of Id2 proteins, concurrent with a loss of Id1 expression, during normal mammary epithelial cell differentiation mirrors the changes observed with TSA-induced differentiation of A2780 cells (Fig. 9).

In epithelial cells, cytokeratin proteins are a significant structural component of the cytoskeleton and are often used as a cytologic marker in the diagnosis and classification of epithelial malignancies (43). TSA induced the reexpression of cytokeratin proteins in A2780 cells (Fig. 6), consistent with epithelial-like differentiation. Reexpression of silenced genes has also been reported in other cancer cell lines (44), including epithelial cancers of the breast, where inhibition of HDACs resulted in increased expression of milk fat globule proteins (45). TSA also induced ultrastructural changes in A2780 cells (Fig. 7), including the formation of primitive intercellular junctions resembling zonulae occluden and macula occluden junctions, and increased the numbers of intercellular luminal spaces containing primitive microvilli. The reexpression of cytokeratins and formation of intercellular junctions provide convincing evidence that TSA induces epithelial-like differentiation of A2780 cells, possibly as the result of a loss of Id1 inhibition of phenotypic gene expression required for epithelial differentiation.

Finally, TSA exposure in another ovarian cancer cell line, SK-OV-3, produced morphological, cell cycle, and differentiation actions similar to those observed in A2780 cells. However, when we examined ovarian cell lines with known resistance to cisplatinum (OVCAR-3 or A2780/CP), we observed none of the morphological or cell cycle-regulatory factor changes observed in the A2780 cells. Instead, TSA induced a strong apoptotic response, as determined by elevated annexin V binding and induction of caspase 3 activity (data not shown). Studies are currently under way to examine

the relationship between TSA-induced apoptosis and cisplatinum resistance in these cell lines.

In conclusion, the actions of TSA in ovarian tumor cells are a clear indication that epigenetic modifications that result from hypoacetylation of histone proteins may play a critical role in the etiology of ovarian cancers by altering the expression of genes involved in cell cycle control and differentiation.

Acknowledgments

We thank Janet Hansen for assistance with the immunohistochemical and EM analyses, Susan Wall for preparation of the paraffin-embedded A2780 cell blocks, Jeffrey G. Anderson for technical assistance in performing flow cytometry, and Dale Kern for computer support in preparation of the manuscript.

References

1. Mant, J. W. F., and Vessey, M. P. Ovarian and endometrial cancers. *In:* R. Doll, J. J. F. Fraumeni, and C. S. Muir (eds.), Trends in Cancer Incidence and Mortality, pp. 287–307. Plainview, NY: Cold Spring Harbor Laboratory, 1994.

2. Weidle, U. H., and Grossmann, A. Inhibition of histone deacetylase: a new strategy to target epigenetic modifications for anticancer treatment. Anticancer Res., *20:* 1471–1486, 2000.

3. Marks, P. A., Richon, V. M., and Rifkind, R. A. Histone deacetylase inhibitors: inducers of differentiation or apoptosis of transformed cells. J. Natl. Cancer Inst. (Bethesda), *92:* 1210–1216, 2000.

4. Grunstein, M. Histone acetylation in chromatin structure and transcription. Nature (Lond.), *389:* 349–352, 1997.

5. Hong, L., Schroth, G. P., Matthews, H. R., Yau, P., and Bradbury, E. M. Studies of the DNA binding properties of histone H4 amino terminus: thermal denaturation studies reveal that acetylation markedly reduces the binding constant of the H4 "tail" to DNA. J. Biol. Chem., *268:* 305–314, 1993.

6. Brownell, J. E., Zhou, J., Ranalli, T., Kobayashi, R., Edmonson, D. G., Roth, S. Y., and Allis, C. D. Tetrahymena histone acetyl-transferase A: a homolog to yeast Gcn5p linking histone acetylation to gene activation. Cell, *84:* 843–850, 1996.

7. Ogryzko, V. V., Schitz, R. L., Russanova, V., Howard, B. H., and Nakatani, Y. The transcriptional coactivators p300 and CBP are histone acetyltransferases. Cell, *87:* 953–958, 1996.

8. Kuo, M. H., and Allis, C. D. Roles of histone acetyltransferases and deacetylases in gene regulation. Bioessays, *20:* 615–621, 1998.

9. Van Lint, C., Emiliani, S., and Verdin, E. The expression of a small fraction of cellular genes is changed in response to histone hyperacetylation. Gene Expr., *5:* 245–253, 1996.

10. Lin, R. J., Egan, D. A., and Evans, R. M. Molecular genetics of acute promyelocytic leukemia. Trends Genet., *15:* 179–184, 1999.

11. Warrel, R. P., He, L. Z., Richon, V. M., Calleja, E., and Pandolfi, P. P. Therapeutic targeting of transcription in acute promyelocytic leukemia by use of an inhibitor of histone deacetylase. J. Natl. Cancer Inst. (Bethesda), *90:* 1621–1625, 1998.

12. Finnin, M. S., Donigian, J. R., Cohen, A., Richon, V. M., Rifkind, R. A., Marks, P. A., Breslow, R., and Pavletich, N. P. Structures of a histone deacteylase homologue bound to the TSA and SAHA inhibitors. Nature (Lond.), *401:* 188–191, 1999.

13. Vigushin, D. M., Ali, S., Pace, P. E., Mirsaidi, N., Ito, K., Adcock, I., and Coombes, R. C. Trichostatin A is a histone deacetylase inhibitor with potent antitumor activity against breast cancer *in vivo*. Clin. Cancer Res., *7:* 971–976, 2001.

14. Della Ragione, F., Criniti, V., Della Pietra, V., Borriello, A., Oliva, A., Indaco, S., Yamamoto, T., and Zappia, V. Genes modulated by histone acetylation as new effectors of butyrate activity. FEBS Lett., *499:* 199–204, 2001.

15. Eickhoff, B., Ruller, S., Laue, T., Kohler, G., Stahl, C., Schlaak, M., and van der Bosch, J. Trichostatin A modulates expression of p21waf1/cip1, Bcl-xL, ID1, ID2, ID3, CRAB2, GATA-2, hsp86 and TFIID/TAFII31 mRNA in human lung adenocarcinoma cells. Biol. Chem., *381:* 107–112, 2000.

16. Ferrara, F. F., Fazi, F., Bianchini, A., Padula, F., Gelmetti, V., Minucci, S., Mancini, M., Pelicci, P. G., Coco, F. L., and Nervi, C. Histone deacetylase-targeted treatment restores retinoic acid signaling and differentiation in acute myeloid leukemia. Cancer Res., *61:* 2–7, 2001.

17. Archer, S. Y., Meng, S., Shei, A., and Hodin, R. A. p21(WAF1) is required for butyrate-mediated growth inhibition of human colon cancer cells. Proc. Natl. Acad. Sci. USA, *95:* 6791–6796, 1998.

18. Harper, J. W., Adami, G. R., Keyomarsi, K., and Elledge, S. J. The p21 Cdk-interacting protein Cip1 is a potent inhibitor of G_1 cyclin-dependent kinases. Cell, *75:* 805–816, 1993.

19. Wang, J. Y. J., Knudsen, E. S., and Welch, P. J. The retinoblastoma tumor suppressor protein. Adv. Cancer Res., *64:* 25–85, 1994.

20. Zebedee, Z., and Hara, E. Id proteins in cell cycle control and cellular senescence. Oncogene, *20:* 8317–8325, 2001.

21. Norton, J. D. ID helix-loop-helix proteins in cell growth, differentiation and tumorigenesis. J. Cell Sci., *113:* 3897–3905, 2000.

22. Benzara, R., Davis, R., Lockshon, D., Turner, D., and Weintraub, H. The protein ID: a negative regulator of helix-loop-helix DNA binding proteins. Cell, *61:* 49–59, 1990.

23. Israel, M. A., Hernandez, M-C., Florio, M., Andres-Barquin, P. J., Mantani, A., Carter, J. H., and Julin, C. M. Id gene expression as a key mediator of tumor cell biology. Cancer Res., *59:* 1726–1730, 1999.

24. Warnick, C. T., Dabbas, B., Ford, C. D., and Strait, K. A. Identification of a p53 response element in the promoter region of the hMSH2 gene required for expression in A2780 ovarian cancer cells. J. Biol. Chem., *276:* 27363–27370, 2001.

25. Sheehy, G. Plasma techniques for minute specimens. J. Histotechnol., *9:* 134–139, 1986.

26. Longnecker, D. S. A program for automated hematoxylin and eosin staining. Am. J. Clin. Pathol., *45:* 229, 1966.

27. Guesdon, J. L., Ternynck, T., and Avrameas, S. The use of avidin-biotin interaction in immunoenzymatic techniques. J. Histochem. Cytochem., *27:* 1131–1139, 1979.

28. Nusse, M., Beisker, W., Hoffman, C., and Tarnok, A. Flow cytometric analysis of G_1- and G_2/M-phase subpopulations in mammalian cell nuclei using side scatter and DNA content measurement. Cytometry, *11:* 813–821, 1990.

29. Erlandson, R. A. Diagnostis Transmission Electron Microscopy of Tumors. New York, NY: Raven Press, 1994.

30. Desprez, P. Y., Hara, E., Bissell, M. J., and Campisi, J. Suppression of mammary epithelial cell differentiation by the helix-loop-helix protein Id-1. Mol. Cell. Biochem., *6:* 3398–3404, 1995.

31. Melichar, B., Ferrandina, G., Verschraegen, C. F., Loercher, A., Abbruzzese, J. L., and Freedman, R. S. Growth inhibitory effects of aromatic fatty acids on ovarian tumor cell lines. Clin. Cancer Res., *4:* 3069–3076, 1998.

32. Ogryzko, V. V., Hirai, T. H., Russanova, V. R., Barbi, D. A., and Howard, B. H. Human fibroblasts commitment to a senescence-like state in response to histone deacetylase inhibitors is cell cycle dependent. Mol. Cell. Biol., *16:* 5210–5218, 1996.

33. Knudsen, E. S., and Wang, J. Y. Differential regulation of the retinoblastoma protein function by specific cdk phosphorylation sites. J. Biol. Chem., *271:* 8313–8320, 1996.

34. Christy, B. A., Sanders, L. K., Lau, L. F., Copeland, N. G., Jenkins, N. A., and Nathans, D. An Id-related helix-loop-helix protein encoded by a growth factor-inducible gene. Proc. Natl. Acad. Sci. USA, *88:* 1815–1819, 1991.

35. Barone, M. V., Pepperkok, R., Peverali, F. A., and Philipson, L. Id proteins control growth induction in mammalian cells. Proc. Natl. Acad. Sci. USA, *91:* 4985–4988, 1994.

36. Inoue, T., Shoji, W., and Obinata, M. MIDA1, an ID-associated protein, has two distinct DNA binding activities that are converted by the associ-

ation with Id1: a novel function of Id protein. Biochem. Biophys. Res. Commun., *266:* 147–151, 1999.

37. Prabhue, S., Ignatova, A., Park, S. T., and Sun, X-H. Regulation of expression of the cyclin dependent kinase inhibitor p21 by E2A and ID proteins. Mol. Cell. Biochem., *17:* 5888–5896, 1997.

38. Melnikova, I. N., Bounpheng, M., Schatteman, G. C., Gilliam, D., and Christy, B. A. Differential biological activities of mammalian Id proteins in muscle cells. Exp. Cell Res., *247:* 94–104, 1999.

39. Hara, E., Hall, M., and Peters, G. Cdk2-dependent phosphorylation of Id2 modulates activity of E2A-related transcription factors. EMBO J., *16:* 332–342, 1997.

40. Ishiguro, A., Konstantin, S., Spirin, M. S., Tobler, A., Gombart, A., Israel, M. A., Norton, J. D., and Keoffler, H. P. Id2 expression increases with differentiation of human myeloid cells. Blood, *87:* 5225–5231, 1996.

41. Condorelli, G., Vitelli, L., Valtieri, M., Marta, I., Montesoro, E., Lulli, V., Baer, R., and Peschle, C. Coordinate expression and developmental role of Id2 protein and TAL1/E2A heterodimer in erythroid progenitor differentiation. Blood, *86:* 164–175, 1995.

42. Parrinello, S., Lin, C. Q., Murata, K., Itahana, Y., Singh, J., Krtolica, A., Campisi, J., and Desprez, P. Y. Id-1, ITF-2, and Id-2 comprise a network of helix-loop-helix proteins that regulate mammary epithelial cell proliferation, differentiation, and apoptosis. J. Biol. Chem., *276:* 39213–39219, 2001.

43. Moll, R., Franke, W. W., Schiller, D. L., Geiger, B., and Krepler, R. The catalog of human cytokeratins: pattern of expression in normal epithelia, tumors and cultured cells. Cell, *31:* 11–24, 1982.

44. Cress, W. D., and Seto, E. Histone deacetylase, transcriptional control, and cancer. J. Cell. Physiol., *184:* 1–16, 2000.

45. Munster, P. M., Troso-Sandoval, T., Rosen, N., Rifkind, R. A., Marks, P. A., and Richon, V. M. The histone deacetylase inhibitor suberoylanilide hydroxamic acid induces differentiation of human breast cancer cells. Cancer Res., *61:* 8492–8497, 2001.